

Phosphorylation of CHIP at Ser20 by Cdk5 promotes tAIF-mediated neuronal death

C Kim^{1,2}, N Yun¹, J Lee¹, MBH Youdim³, C Ju⁴, W-K Kim⁴, P-L Han^{*2} and YJ Oh^{*1}

Cyclin-dependent kinase 5 (Cdk5) is a proline-directed serine/threonine kinase and its dysregulation is implicated in neurodegenerative diseases. Likewise, C-terminus of Hsc70-interacting protein (CHIP) is linked to neurological disorders, serving as an E3 ubiquitin ligase for targeting damaged or toxic proteins for proteasomal degradation. Here, we demonstrate that CHIP is a novel substrate for Cdk5. Cdk5 phosphorylates CHIP at Ser20 via direct binding to a highly charged domain of CHIP. Co-immunoprecipitation and ubiquitination assays reveal that Cdk5-mediated phosphorylation disrupts the interaction between CHIP and truncated apoptosis-inducing factor (tAIF) without affecting CHIP's E3 ligase activity, resulting in the inhibition of CHIP-mediated degradation of tAIF. Lentiviral transduction assay shows that knockdown of Cdk5 or overexpression of CHIP^{S20A}, but not CHIP^{WT}, attenuates tAIF-mediated neuronal cell death induced by hydrogen peroxide. Thus, we conclude that Cdk5-mediated phosphorylation of CHIP negatively regulates its neuroprotective function, thereby contributing to neuronal cell death progression following neurotoxic stimuli.

Cell Death and Differentiation (2016) 23, 333–346; doi:10.1038/cdd.2015.103; published online 24 July 2015

Cyclin-dependent kinase 5 (Cdk5) is a member of cyclin-dependent kinase that is crucial for the regulation of various post-mitotic cellular processes in the nervous system.^{1–4} Although Cdk5 is activated upon direct interaction with a neural-specific activator p35 in normal condition,¹ it can be hyperactivated in numerous pathological conditions by the conversion of p35 to p25 via calpain.⁵ Therefore, dysregulation of Cdk5 activity has been linked to an array of neurodegenerative diseases.^{2,5,6} Consequently, Cdk5-mediated phosphorylation of several key intracellular substrates has received significant attention and has been identified to associate with the pathophysiology of neurodegeneration.^{6,7}

Recently, our laboratory made an attempt to identify the novel substrate of Cdk5 and we came across that Cdk5 interacts with C-terminus of Hsc70-interacting protein (CHIP). CHIP is composed of three major domains: (1) an amino-terminal three tetratricopeptide repeat (TPR) domain interacting with Hsc/Hsp70 and Hsp90, (2) a highly charged central domain with unknown functions and (3) a carboxyl-terminal U-box domain conferring E3 ubiquitin ligase activity.^{8–10} Based on these domains, it has been indicated that CHIP has a crucial role as a molecular co-chaperone in the maintenance of protein homeostasis during cellular stress and recovery.^{8,11–13} Indeed, CHIP has been demonstrated to serve as a crucial catalyst for ubiquitination of Hsp70 client

proteins targeting for proteasome-dependent degradation.¹¹ The function of CHIP with its molecular chaperones has been well documented to reduce cellular toxicity associated with several neurodegenerative diseases.^{11,12,14–18} However, the mechanisms underlying how function of CHIP is regulated and, if any, the pathophysiological cascades contributing to CHIP-mediated neurodegeneration are not fully elucidated yet.

Here, we propose the molecular cascade in which Cdk5 phosphorylation of CHIP at Ser20 disrupts the interaction between CHIP and truncated apoptosis-inducing factor (tAIF), thereby contributes to escaping of tAIF from CHIP-mediated proteasome-dependent degradation, and eventually leads to tAIF-mediated neuronal cell death. We argue that this cascade explains one plausible mechanism as to how dysregulation of Cdk5 leads to neuronal death by negatively regulating CHIP-mediated degradation of toxic molecules.

Results

Cdk5 phosphorylates CHIP at Ser20. Bioinformatic analysis revealed the presence of putative Cdk5-mediated phosphorylation sites on the CHIP protein (Supplementary Table 1). To determine whether Cdk5 phosphorylates CHIP, we performed an *in vitro* kinase assay by incubating the

¹Department of Systems Biology, Yonsei University College of Life Science and Biotechnology, Seoul 120-749, Korea; ²Department of Brain and Cognitive Sciences, Ewha Womans University, Seoul 120-750, Korea; ³Technion Rapport Faculty of Medicine, Eve Topf and NPF Centers of Excellence for Neurodegenerative Diseases Haifa, Haifa 30196, Israel and ⁴Department of Neuroscience, College of Medicine, Korea University, Seoul 136-705, Korea

*Corresponding author: P-L Han, Department of Brain and Cognitive Sciences, Ewha Womans University, Seoul 120-750, Korea. Tel: +82 2 3277 4130; Fax: +82 2 3277 6931; E-mail: plhan@ewha.ac.kr

or YJ Oh, Department of Systems Biology, Yonsei University College of Life Science and Biotechnology, Seoul 120-749, Korea. Tel: +82 2 2123 2662; Fax: +82 2 312 5657; E-mail: yjoh@yonsei.ac.kr

Abbreviations: Cdk5, cyclin-dependent kinase 5; CHIP, C-terminus of Hsc70-interacting protein; tAIF, truncated apoptosis-inducing factor; TPR, tetratricopeptide repeat; GST, glutathione S-transferase; HA, hemagglutinin; WT, wild type; KD, kinase-dead; CIP, calf intestinal alkaline phosphatase; UPS, ubiquitin proteasome system; MEF, mouse embryonic fibroblast; MTT, 3-(4,5-dimethylthiazol-2-yl)-2,5-diphenyltetrazolium bromide; shRNA, short hairpin RNA; CBB, Coomassie brilliant blue; Co-IP, co-immunoprecipitation

Received 23.2.15; revised 29.5.15; accepted 23.6.15; Edited by L. Greene; published online 24.7.15

purified glutathione S-transferase (GST)-CHIP protein with the purified complex of Cdk5 and p25. We found that CHIP was phosphorylated in the presence of the Cdk5/p25 complex, whereas Cdk5-mediated phosphorylation of CHIP was dose-dependently abrogated by roscovitine, a selective Cdk5 inhibitor (Figure 1a). To examine whether Cdk5 phosphorylates CHIP *in vivo*, HEK293 cells were transfected with hemagglutinin (HA)-CHIP in combination with Flag-Cdk5

wild type (WT) plus p25-Myc (Flag-Cdk5 WT/p25-Myc) or Flag-Cdk5 kinase-dead (KD; D144N, a catalytically inactive mutant) plus p25-Myc (Flag-Cdk5 KD/p25-Myc). Cdk5-mediated phosphorylation caused an upward shift of the CHIP band, whereas this phenomenon was not detected in cells expressing Cdk5 KD (Figure 1b). We confirmed this finding in neuronal cell lines (Supplementary Figure 1). Cdk5/p25-mediated upward shift of CHIP band was returned to the

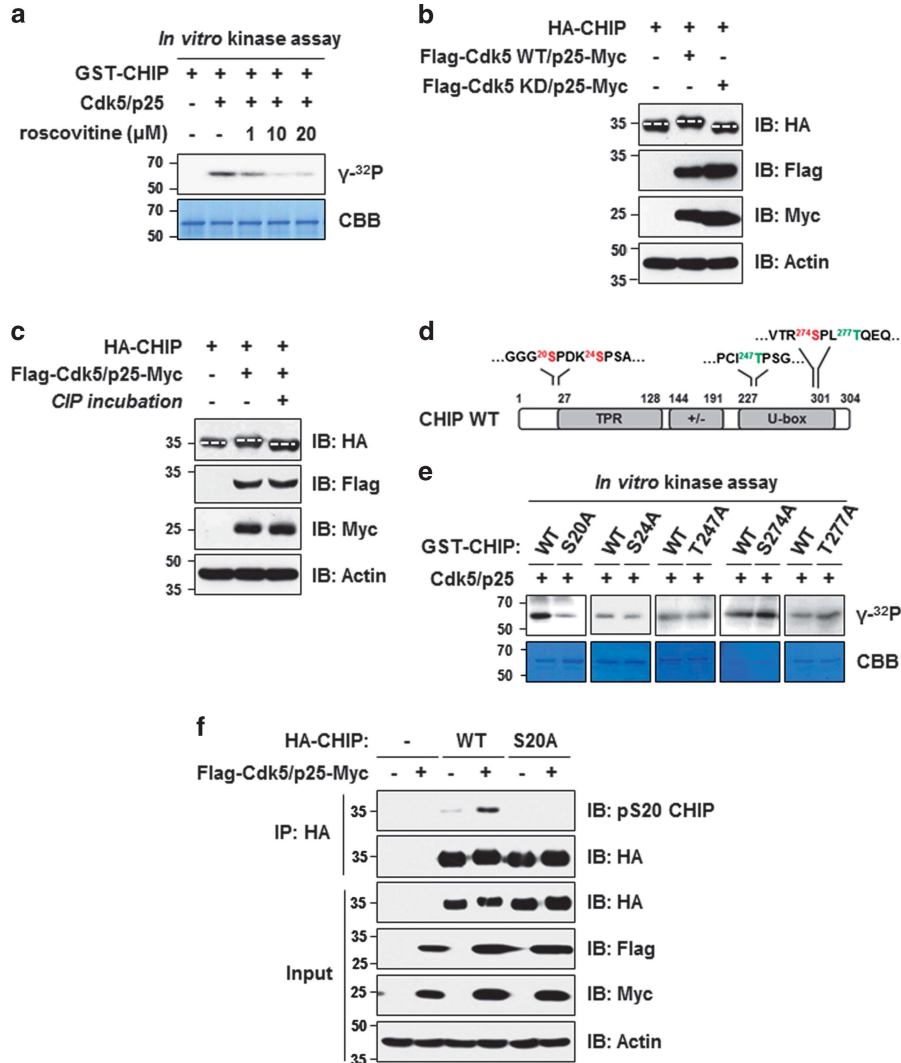


Figure 1 Cdk5 phosphorylates CHIP at Ser20. (a) Recombinant GST-CHIP protein (3 μ g) was incubated with the purified active Cdk5/p25 kinase complex (0.5 μ g) in the presence of [γ -³²P]ATP plus indicated doses of roscovitine, a selective Cdk5 inhibitor. The reaction products were resolved by SDS-PAGE and subjected to autoradiography. Coomassie brilliant blue (CBB) staining for GST-CHIP protein was provided at the bottom and used as a loading control. (b) HEK293 cells were transfected with HA-CHIP in combination with either Flag-Cdk5 WT/p25-Myc or Flag-Cdk5 KD/p25-Myc. Cell lysates were resolved by SDS-PAGE followed by immunoblot (IB) analysis using the indicated antibodies. Positions of the phosphorylated and non-phosphorylated HA-CHIP were indicated by the white dotted lines. Actin antibody was used as a loading control. (c) Following transfection of HEK293 cells with HA-CHIP and Flag-Cdk5/p25-Myc, cell lysates were incubated with calf intestinal alkaline phosphatase (CIP). The reaction products were subjected to IB analysis using the indicated antibodies. (d) Schematic representation of the putative phosphorylation sites on CHIP obtained from bioinformatic analyses through the computational databases depicted in Supplementary Table 1. Three putative serine (S) phosphorylation sites (red) and two putative threonine (T) phosphorylation sites (green) are indicated. TPR, tetratricopeptide repeat domain; +/-, highly charged domain; U-box, E3 ligase domain. (e) Recombinant GST-CHIP WT (3 μ g) or other phospho-null mutant proteins (S20A, S24A, T247A, S274A and T277A; 3 μ g each) was incubated with the purified, active Cdk5/p25 kinase complex (0.5 μ g) in the presence of [γ -³²P]ATP. The reaction products were resolved by SDS-PAGE and subjected to autoradiography. (f) Antibodies specifically recognizing the phosphorylated Ser20 site (pS20 CHIP) were raised from the peptide sequences, TGGG(pS)PDKSP surrounding the Ser20 residue of mouse CHIP. The specificity of the antibody was confirmed by the absence of the corresponding band in immunoprecipitation (IP) analysis using the cell lysates from HEK293 cells transiently expressing HA-CHIP S20A in combination with Flag-Cdk5 WT/p25-Myc when compared with that of wild type

corresponding non-phosphorylated position when incubated with calf intestinal alkaline phosphatase (CIP; Figure 1c). Given that CHIP has five putative phosphorylation sites (Figure 1d and Supplementary Table 1), we carried out an *in vitro* kinase assay to assess the actual phosphorylation site of CHIP by incubating the Cdk5/p25 complex with each of the indicated purified GST-CHIP proteins. The extent of phosphorylation considerably decreased in a CHIP S20A mutant, but not in other CHIP mutants as compared with that in CHIP WT (Figure 1e). The identified Ser20 site on CHIP resides in (S/T)PX(K/R), the highly conserved consensus sequence for the phosphorylation across species (Supplementary Figure 2).^{19–21} To further confirm whether Cdk5 phosphorylates CHIP at Ser20 *in vivo*, we raised a rabbit polyclonal antibody and confirmed its specificity (Supplementary Figure 3). Indeed, this antibody detected the phosphorylated CHIP at Ser20 in HEK293 cells expressing both HA-CHIP WT and Flag-Cdk5/p25-Myc (Figure 1f). No such phosphorylation was detected in HEK293 cells expressing a HA-CHIP S20A mutant (a phospho-null mutant). Thus, we argue that Cdk5 specifically phosphorylates CHIP at Ser20.

Previous reports indicated that both CHIP and Cdk5 are highly expressed in the brain.^{2,9,12} Thus, we tested whether Cdk5-mediated phosphorylation of CHIP can be interpreted as a consequence of a direct interaction between these two proteins. A reciprocal co-immunoprecipitation (co-IP) analysis as well as an immunofluorescence analysis indicated that Cdk5 is co-localized and interacts with CHIP (Figures 2a and b). No obvious difference in their interactive capacity was detected in HEK293 cells expressing Flag-Cdk5 WT or Flag-Cdk5 KD (Figure 2c), indicating that kinase activity is not necessary for their binding. Indeed, a reciprocal co-IP analysis using cell lysates obtained from HEK293 cells and mouse brain extracts demonstrated that Cdk5 interacts with CHIP (Figures 2d and e), indicating endogenous binding of these two proteins. A pull-down assay demonstrated that Cdk5, but not p35 and p25, directly interacts with CHIP (Figure 2f). To map the critical domain of CHIP necessary for its interaction with Cdk5, we performed co-IP analysis and found that Cdk5 interacts with CHIP lacking the TPR or U-box domain, but not with CHIP lacking the highly charged domain (Supplementary Figure 4).

Cdk5-mediated phosphorylation of CHIP at Ser20 negatively regulates tAIF degradation via ubiquitin proteasome system (UPS). The neuroprotective functions of CHIP have been attributed to its regulation of substrate stability via UPS.^{11,22–27} Recently, it has been demonstrated that one of representative example is tAIF.²⁸ In this report, CHIP was found to attenuate tAIF-mediated cell death by directly binding to and targeting it to UPS. These findings prompted us to address whether Cdk5-mediated phosphorylation of CHIP affects the rate of tAIF degradation. Immunoblot analysis indicated that levels of the ectopically expressed tAIF significantly decreased by CHIP, whereas its level was restored when CHIP was phosphorylated by Cdk5 WT (Figure 3a, lanes 1–3). In contrast, CHIP-mediated decreased level of tAIF was not restored in Cdk5 KD-expressing HEK293 cells (Figure 3a, lane 4). This phenomenon was confirmed in neuronal cell

lines (Supplementary Figure 5), supporting that Cdk5-mediated phosphorylation of CHIP may negatively regulate CHIP-mediated degradation of tAIF. Next, we wondered whether ectopically expressed tAIF is similarly regulated in CHIP WT (+/+) and knockout (KO; –/–)-derived mouse embryonic fibroblasts (MEFs) expressing Flag-Cdk5/p25-Myc. We found that a decrease of tAIF level was detected in CHIP (+/+) MEF cells, but not in CHIP (–/–) MEF cells (Figure 3b, lane 1 *versus* lane 3). This phenomenon was significantly blocked in CHIP (+/+) MEF cells in which phosphorylation of CHIP at Ser20 was manifested by overexpressed Cdk5 and p25 (Figure 3b, lane 2). As expected, no obvious change in levels of tAIF was detected in CHIP (–/–) MEF cells regardless of overexpression of Cdk5 and p25 (Figure 3b, lane 3 *versus* lane 4). To further ascertain whether the tAIF degradation is specifically regulated by Cdk5-mediated phosphorylation of CHIP at Ser20, HA-CHIP WT or CHIP S20A was reintroduced into the CHIP (–/–) MEF cells and levels of tAIF were accordingly monitored. We found that reintroduction of CHIP WT or CHIP S20A into CHIP (–/–) MEF cells led to decreased levels of tAIF (Figure 3c, lane 2 and lane 4). This CHIP-mediated decrease of tAIF level was significantly blocked by the expression of Cdk5/p25 complex in CHIP (–/–) MEF cells expressing CHIP WT, but not in CHIP S20A-expressing cells (Figure 3c, lane 3 *versus* lane 5). In addition, CHIP-mediated tAIF degradation was significantly attenuated in CHIP (–/–) MEF cells that were transfected with CHIP S20D (a phosphomimetic mutant; Supplementary Figure 6a). To address the emerging questions of whether phosphorylation of CHIP by Cdk5 inhibits CHIP-mediated tAIF degradation via UPS, we monitored the ubiquitination pattern of tAIF using HEK293 cells expressing CHIP WT and either Cdk5 WT/p25 or Cdk5 KD/p25. CHIP-mediated tAIF ubiquitination was effectively inhibited in co-expression of CHIP and Cdk5 WT/p25, but not in co-expression of CHIP and Cdk5 KD/p25 (Figure 3d). To pinpoint whether Cdk5-mediated phosphorylation of CHIP at Ser20 is necessary for this event, CHIP-mediated tAIF ubiquitination was compared in HEK293 cells overexpressing Cdk5/p25 in combination with either CHIP WT or CHIP S20A. Ubiquitination of tAIF by CHIP WT was inhibited in Cdk5/p25 expression, whereas CHIP S20A had no effect on CHIP-mediated tAIF ubiquitination (Figure 3e). Furthermore, CHIP-mediated tAIF ubiquitination was attenuated in HEK293 cells overexpressing CHIP S20D (Supplementary Figure 6b), supporting the notion that Cdk5-mediated phosphorylation of CHIP at Ser20 negatively regulates the tAIF degradation via UPS.

Cdk5-mediated phosphorylation of CHIP at Ser20 inhibits the interaction with tAIF without affecting CHIP's E3 ligase activity. Our data can be interpreted as a consequence of either loss of CHIP's E3 ligase activity or other unknown mechanisms. Based on the previous evidence supporting that the phosphorylation of E3 ligases by kinases regulates its ligase activity,^{29–32} therefore, we first attempted to check whether Cdk5-mediated phosphorylation affects CHIP's E3 ligase activity. Auto-ubiquitination assay was conducted to measure E3 ligase activity (Figures 4a and b). *In vitro* kinase assay was conducted by incubating GST-CHIP

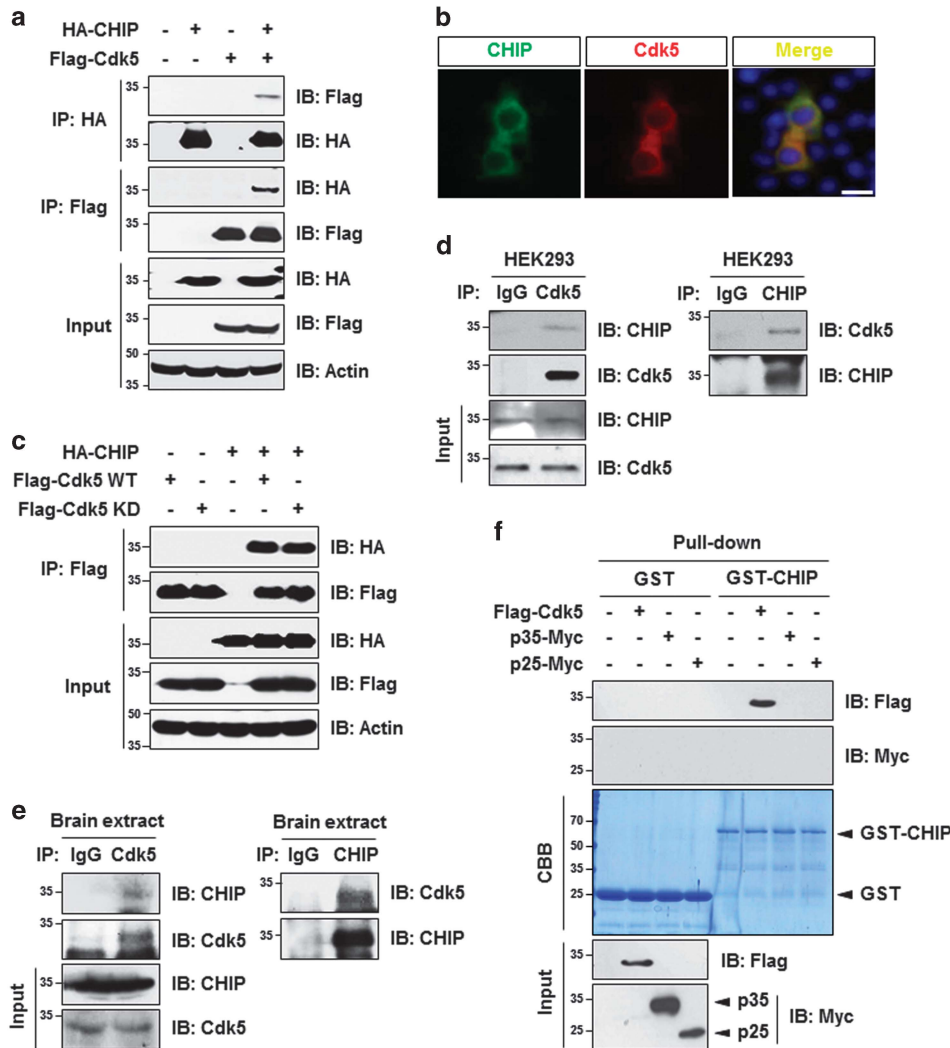


Figure 2 Cdk5 interacts with CHIP. (a) Following transfection of HEK293 cells with HA-CHIP or Flag-Cdk5 alone or in combination, cell lysates were collected for IP using anti-HA antibody or Flag-conjugated beads, respectively. Immunoprecipitates or inputs were resolved by SDS-PAGE and subjected to IB analysis using the indicated antibodies. (b) HEK293 cells transfected with HA-CHIP (green) and Cdk5-DsRed2 (red) were subjected to immunofluorescent co-localization analysis and examined under a confocal microscope. Hoechst 33258 was used to visualize the nuclei. Merged image was provided. Scale bar represents 10 μ m. (c) Cell lysates from HEK293 cells transfected with HA-CHIP alone or in combination with Flag-Cdk5 WT or KD mutant were collected for IP by Flag-conjugated bead. Signals from the immunoprecipitates or inputs were measured by IB analysis using the indicated antibodies. (d and e) HEK293 cell lysates (d) and tissue extracts (e) from the mouse whole brain were immunoprecipitated for Cdk5 or CHIP using the respective antibodies followed by IB analysis using the indicated antibodies. IgG was used as an immunological control. (f) For *in vitro* pull-down assays, recombinant GST or GST-CHIP was incubated with the indicated cell lysates harvested from HEK293 cells transiently expressing Flag-Cdk5, p35-Myc or p25-Myc alone. After incubation, samples were precipitated by GST-Sepharose beads, and the eluted proteins or inputs were subjected to IB analysis using the indicated antibodies. Coomassie brilliant blue staining was performed to reveal the levels of GST and GST-CHIP proteins (arrow heads) in each lane

proteins with or without Cdk5/p25 complex. A subsequent *in vitro* ubiquitination assay was performed in combination with the presence or the absence of ubiquitin mixture. E3 ligase activity of CHIP was not altered regardless of the state of Cdk5-mediated phosphorylation of CHIP at Ser20 (Figure 4a). To further confirm this phenomenon *in vivo*, we performed denatured IP analysis using HEK293 cells expressing CHIP WT in combination with or without Cdk5/p25. In consistent with *in vitro* data, auto-ubiquitination of CHIP was not changed regardless of its phosphorylated state (Figure 4b), indicating that regulation of CHIP-mediated tAIF degradation by UPS is not due to the alteration of CHIP's E3 ligase activity following phosphorylation by Cdk5.

Accumulated evidences showed that phosphorylation can increase or decrease the rate of protein-protein interaction.^{28,33-36} To investigate whether altered interactions between CHIP and tAIF depends on the Cdk5-mediated phosphorylation state of CHIP, we performed co-IP analysis. Interaction between CHIP and tAIF was inhibited by the expression of Cdk5 WT/p25, but not by Cdk5 KD/p25 (Figure 4c). To further investigate whether Cdk5-mediated phosphorylation of CHIP at Ser20 specifically inhibits the interaction between CHIP and tAIF, we performed co-IP analysis using HEK293 cells overexpressing CHIP (either WT or CHIP S20A) and Cdk5 WT/p25. When Cdk5/p25 were expressed, interaction between CHIP and tAIF was not

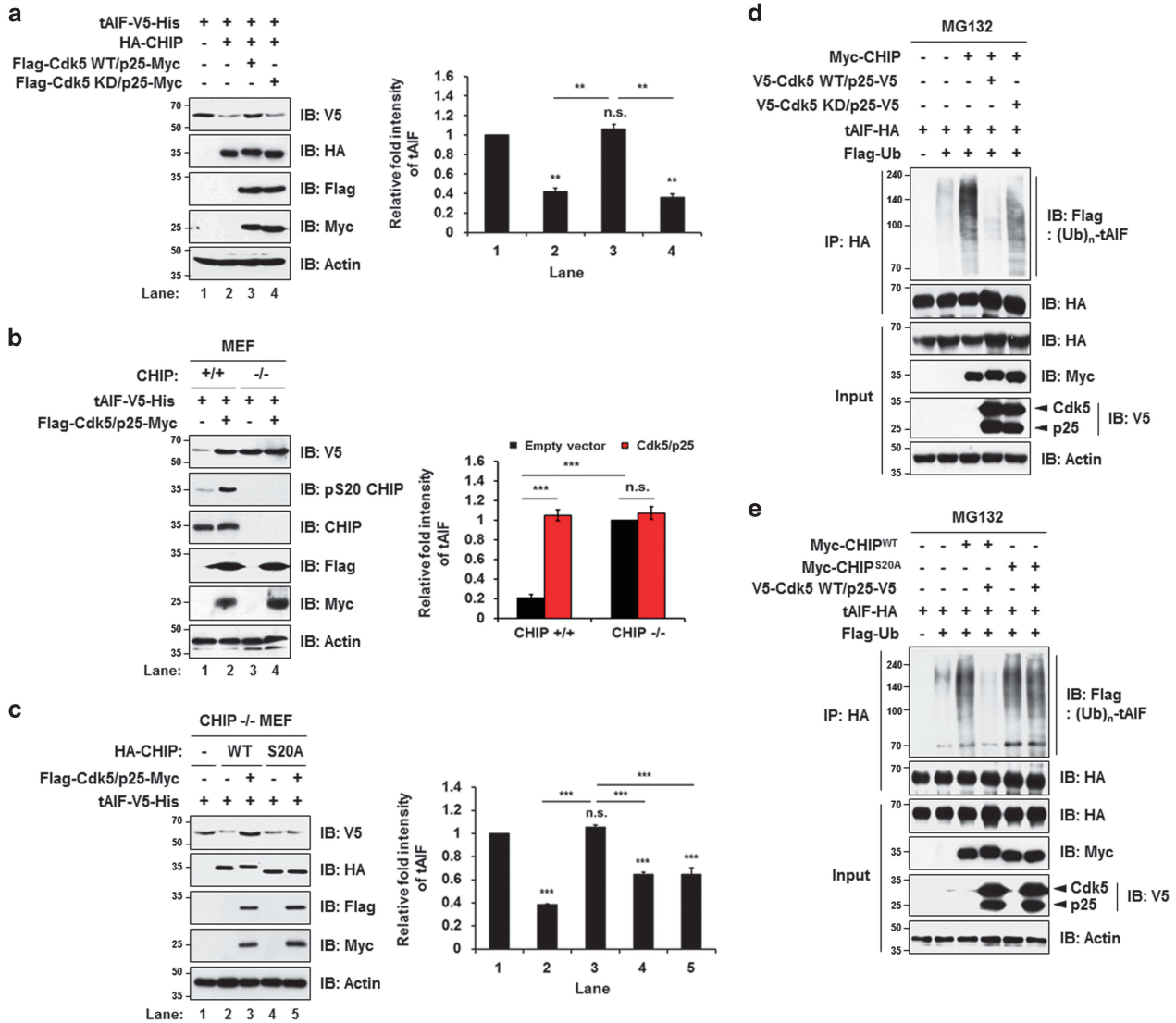


Figure 3 Cdk5 negatively regulates CHIP-mediated tAIF degradation via UPS. (a) Lysates harvested from HEK293 cells expressing tAIF-V5-His alone or in combination with HA-CHIP plus Flag-Cdk5 WT/p25-Myc or KD/p25-Myc were subjected to SDS-PAGE and subsequent IB analysis using the indicated antibodies. After normalization against actin, relative levels of tAIF were expressed as a fold intensity over the control (value = 1; lane 1). Bar represents the means \pm S.D. of three independent experiments. $**P < 0.01$; NS, not significant. (b) Cell lysates harvested from CHIP wild-type (+/+) and knockout (-/-) mouse embryonic fibroblasts (MEFs) expressing tAIF-V5-His alone or in combination with Flag-Cdk5 WT/p25-Myc were subjected to SDS-PAGE followed by IB analysis using the indicated antibodies. After normalization against actin, relative levels of tAIF were expressed as a fold intensity over the control (value = 1; lane 3). Bar represents the means \pm S.D. of three independent experiments. $***P < 0.001$; NS, not significant. (c) CHIP knock out (-/-) MEF cells were transfected with HA-CHIP (either WT or S20A) and tAIF-V5-His along with or without Flag-Cdk5/p25-Myc. Cell lysates were subjected to SDS-PAGE and subsequent IB analysis using the indicated antibodies. After normalization against actin, relative levels of tAIF were expressed as a fold intensity over the control (value = 1; lane 1). Bar represents the means \pm S.D. of three independent experiments. $***P < 0.001$; NS, not significant. (d) HEK293 cells were transfected with the indicated combination of constructs and further maintained for 8 h in media containing 10 μ M MG132. After IP using anti-HA antibody, immunoprecipitates and inputs were subjected to IB analysis using the indicated antibodies. Pattern of the ubiquitinated tAIF was probed with anti-Flag antibody. (e) HEK293 cells were transfected with Myc-CHIP WT or Myc-CHIP S20A along with the indicated combination of constructs, and further maintained for 8 h in media containing 10 μ M MG132. Cell lysates were subjected to IP using anti-HA antibody and IB analysis using the indicated antibodies

inhibited in HEK293 cells overexpressing CHIP S20A as compared with HEK293 cells overexpressing CHIP WT (Figure 4d). In support of these findings, we additionally found that the interaction between CHIP and tAIF was also inhibited in HEK293 cells overexpressing CHIP S20D alone (Supplementary Figure 6c), indicating that phosphorylation of CHIP at Ser20 by Cdk5 inhibits the interaction between CHIP and tAIF, leading to attenuation of CHIP-mediated tAIF degradation via UPS.

Phosphorylation of CHIP at Ser20 by Cdk5 activation promotes neuronal cell death following hydrogen peroxide treatment. Cdk5 activation is increased by cleavage of its regulatory protein p35 to p25 in response to neurotoxic insults.^{37,38} Given the emerging link between both Cdk5 and tAIF and oxidative stress-induced neuronal cell death,³⁹⁻⁴² we hypothesized that oxidative stress-induced Cdk5 activation triggers neuronal cell death by inhibiting CHIP-mediated degradation of tAIF. In primary cultured

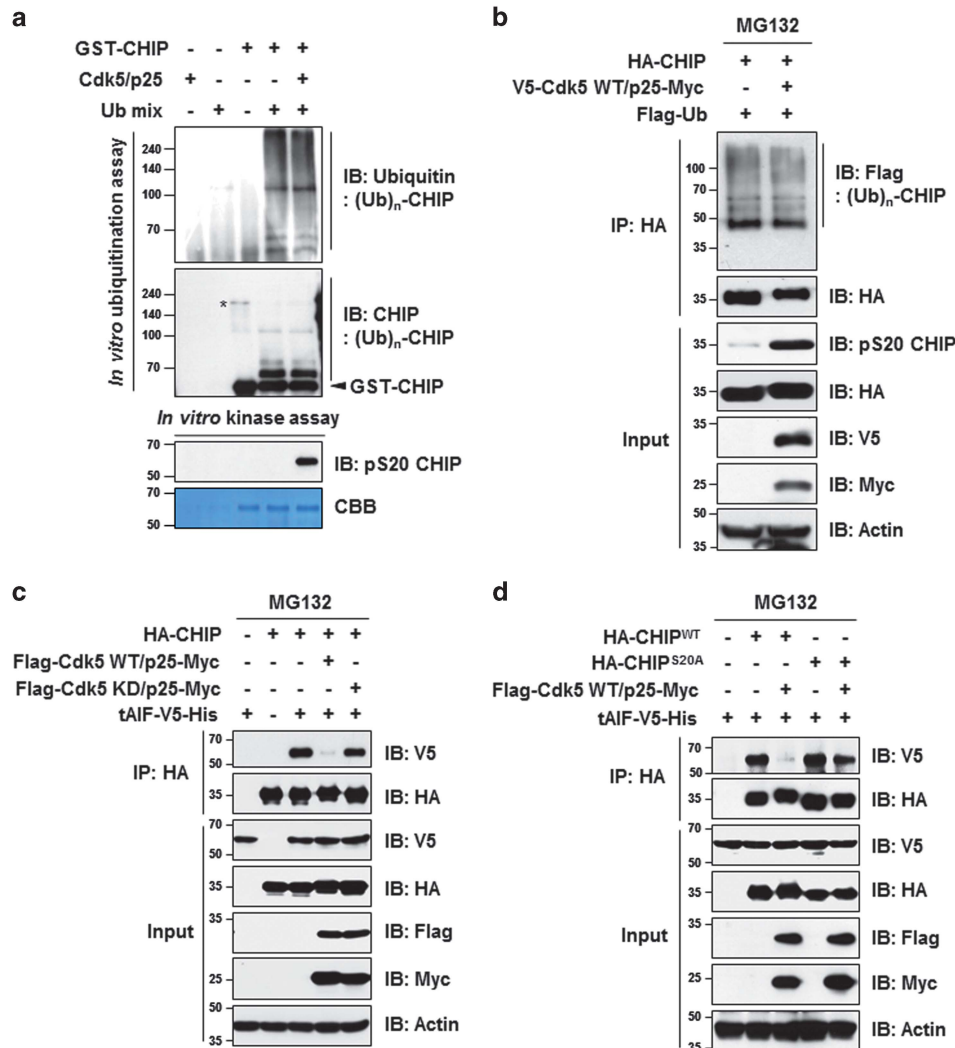


Figure 4 Cdk5-mediated phosphorylation of CHIP at Ser20 disrupts the interaction with tAIF. (a) (Bottom panel) For *in vitro* kinase assay, GST-CHIP proteins (3 μ g) were incubated with the purified active Cdk5/p25 kinase complex (0.5 μ g). (Top panel) The reaction products were further incubated with or without ubiquitin mixture (Ub mix; including UBE1 (as E1 enzyme), UbcH5b (as E2 enzyme) and ubiquitin) for *in vitro* ubiquitination assay. Each reaction products were subjected to IB analysis using the indicated antibodies. Coomassie brilliant blue (CBB) staining for GST-CHIP proteins was also provided. The asterisk indicates a nonspecific band. (b) HEK293 cells expressing the indicated combination of HA-CHIP WT, Flag-Ub and V5-Cdk5 WT/p25-Myc were maintained for 8 h in the presence of 10 μ M MG132, a proteasome inhibitor. Cell lysates obtained under a denatured condition were subjected to IP analysis using anti-HA antibody followed by IB analysis using the indicated antibodies. Actin antibody was used as a loading control. (c) HEK293 cells were transfected with the indicated combination of constructs, and further maintained for 8 h in media containing 10 μ M MG132. Cell lysates were collected for IP analysis using anti-HA antibody followed by IB analysis using the indicated antibodies. (d) HEK293 cells transfected with HA-CHIP (either WT or S20A) and tAIF-V5-His together with or without Flag-Cdk5 WT/p25-Myc were maintained for 8 h in media containing 10 μ M MG132. Cell lysates were subjected to IP analysis using anti-HA antibody and IB analysis using the indicated antibodies

cortical neurons, hydrogen peroxide increased levels of tAIF in a time-dependent manner (Figures 5a and c). This event came along with an increased cleavage of p35 into p25 as well as augmented phosphorylation of CHIP at Ser20 (Figures 5a and b). These changes were paralleled with a time-dependent activation of Cdk5 (Figure 5a, bottom panel). Next, we tried to determine whether Cdk5 activation directly regulates phosphorylation of CHIP at Ser20 and the formation of tAIF in hydrogen peroxide-treated cortical neurons. Roscovitine inhibited hydrogen peroxide-induced generation of both phosphorylated CHIP at Ser20 and tAIF, whereas it did not affect the levels of CHIP, Cdk5 and p25 (Figures 5d and e). Next, we attempted to determine whether

this event is linked to cortical neuronal death. We performed two methodologically unrelated assays: large-scale DNA fragmentation and 3-(4,5-dimethylthiazol-2-yl)-2,5-diphenyltetrazolium bromide (MTT) reduction assay. We found that tAIF-mediated generation of 50 kbp DNA fragments increased in hydrogen peroxide-treated cortical neurons and this was significantly inhibited by roscovitine (Figure 5f). MTT reduction assay also demonstrated that hydrogen peroxide-induced neuronal death was attenuated by cotreatment with roscovitine (Figure 5g).

To further confirm role for Cdk5 activation, we set out lentiviral transduction system to knockdown Cdk5 by using two independent short hairpin RNA (shRNA) sequences targeting

Cdk5. As depicted in Figure 6a, cortical neurons were transduced with empirically determined amounts of lentivirus at 7 days *in vitro*, incubated for additional 4 days and exposed

to hydrogen peroxide for 60 min. As compared with a scrambled shRNA, lentivirally expressed shRNAs targeting Cdk5 (Cdk5 #1 and #2) decreased levels of phosphorylated

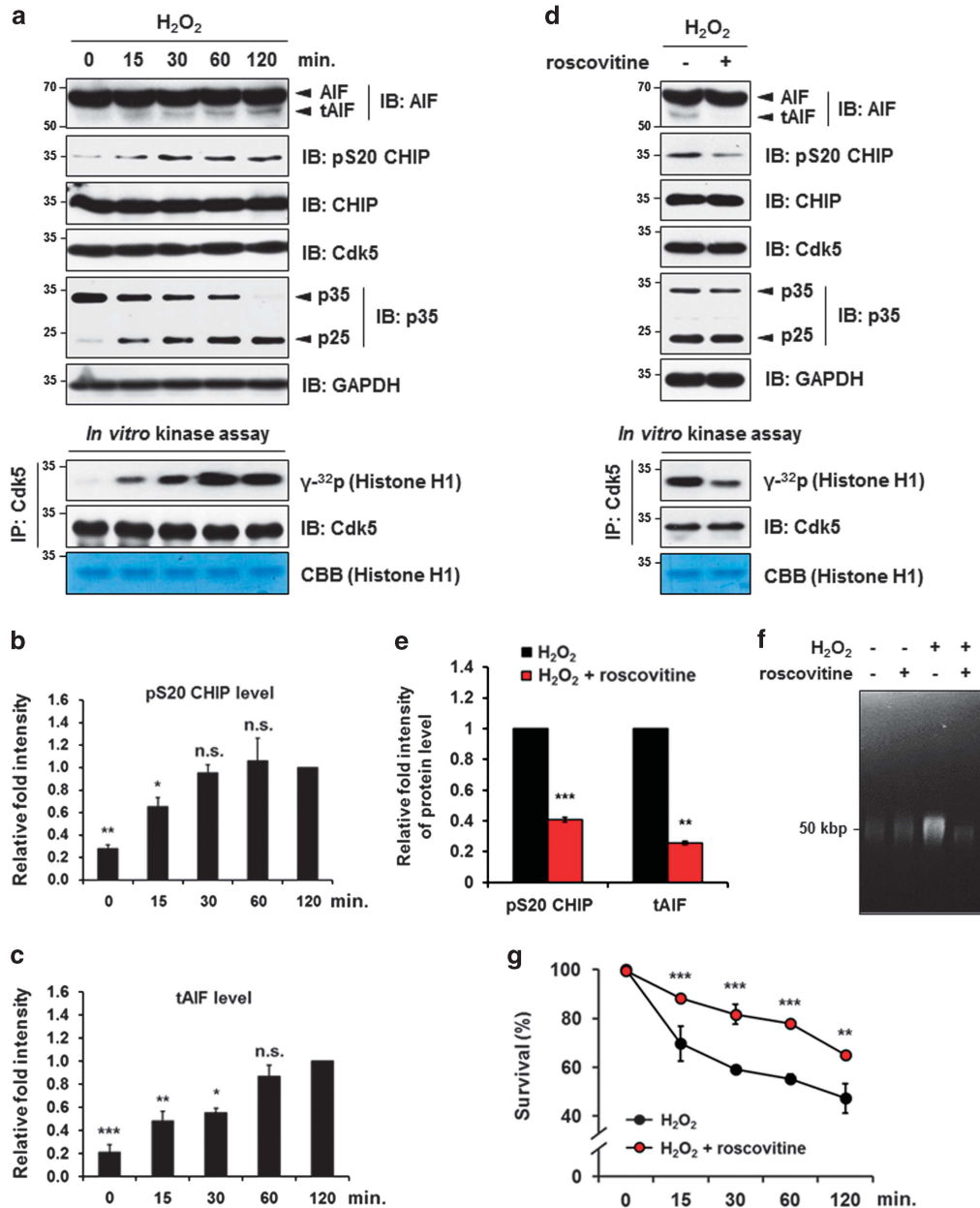


Figure 5 Hydrogen peroxide leads to tAIF-induced neuronal cell death via Cdk5-mediated phosphorylation of CHIP at Ser20. (a) Following treatment of primary cultures of cortical neurons with 200 μ M hydrogen peroxide (H₂O₂) for the indicated time periods, cell lysates were harvested and subjected to IB analysis using the indicated antibodies. For *in vitro* kinase assay, immunoprecipitates with anti-Cdk5 antibody were reacted with 1 μ g Histone H1 in the presence of [γ -³²P]ATP at 30 °C for 30 min. The reaction products were resolved by SDS-PAGE and subjected to autoradiography. Coomassie brilliant blue (CBB)-stained gel represents the level of Histone H1 in each lane. (b and c) After normalization against glyceraldehyde-3-phosphate dehydrogenase (GAPDH), relative levels of (b) pS20 CHIP and (c) tAIF were expressed as a fold intensity over the levels found in cells treated with H₂O₂ for 120 min (value = 1). Bar represents the means \pm S.D. of three independent experiments. **P* < 0.05; ***P* < 0.01; ****P* < 0.001; NS, not significant. (d) Cell lysates harvested from hydrogen peroxide-treated cortical neurons (200 μ M for 60 min) in the presence or the absence of 10 μ M roscovitine were subjected to IB analysis using the indicated antibodies. *In vitro* kinase assay was performed as described in (a). (e) After normalization against GAPDH, relative levels of pS20 CHIP and tAIF were expressed as a fold intensity over the levels found in cells treated with H₂O₂ alone (value = 1). Bar represents the means \pm S.D. of three independent experiments. ***P* < 0.01; ****P* < 0.001. (f) Cortical neurons cultivated for 60 min in the indicated conditions (200 μ M H₂O₂, 10 μ M roscovitine) were subjected to the large-scale DNA fragmentation assay by using a pulsed-field gel electrophoresis. (g) Cortical neurons were exposed to 200 μ M H₂O₂ for the indicated time periods in the presence or the absence of 10 μ M roscovitine. The rate of cell viability was determined by MTT reduction assay. Values are expressed as a percent survival over the untreated control cultures (100%). Data represent the means \pm S.E.M. from three independent experiments done in triplicate. ***P* < 0.01; ****P* < 0.001

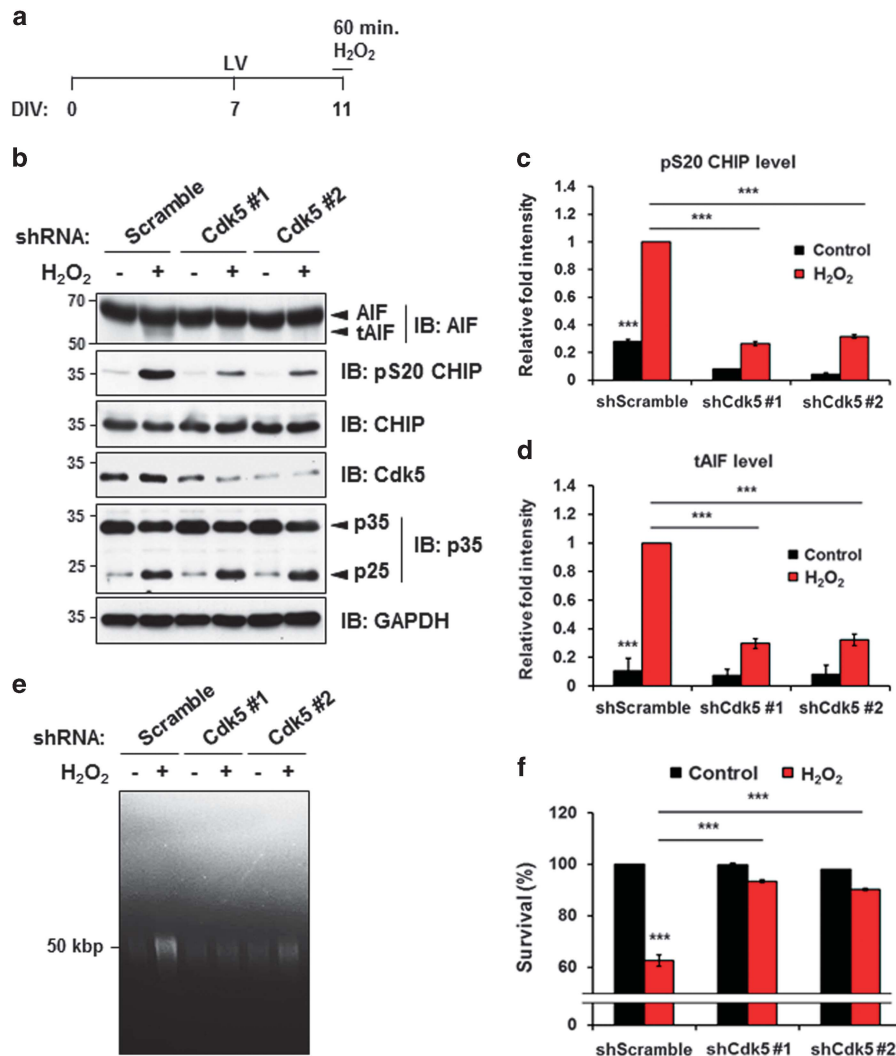


Figure 6 Lentiviral-mediated knockdown of Cdk5 attenuates hydrogen peroxide-mediated neuronal cell death via regulation of tAIF level. (a) Schematic flow for lentiviral transduction (LV) and H₂O₂ treatment. (b) Cortical neurons were infected with lentiviral particles containing shRNA against either Cdk5 (Cdk5 #1 or #2) or control (Scramble) and subsequently treated with 200 μ M H₂O₂ for 60 min. Cell lysates were subjected to IB analysis using the indicated antibodies. (c and d) Quantification of the relative fold intensities of (c) pS20 CHIP and (d) tAIF level was performed and normalized against glyceraldehyde-3-phosphate dehydrogenase (GAPDH). The relative levels were expressed as a fold intensity over H₂O₂-treated controls (shScramble; value = 1). Bar represents the means \pm S.D. of three independent experiments. *** P < 0.001. (e and f) Cortical neurons expressing shRNA to scramble (Scramble) or Cdk5 (Cdk5 #1 and #2) treated with 200 μ M H₂O₂ for 60 min were subjected to (e) the large-scale DNA fragmentation assay by pulsed-field gel electrophoresis and (f) MTT reduction assay. Values are expressed as a percent survival over untreated controls (shScramble). Data represent the means \pm S.E.M. from three independent experiments done in triplicate. *** P < 0.001

CHIP at Ser20 and tAIF without affecting CHIP expression and cleavage of p35 into p25 in hydrogen peroxide-treated cortical neurons (Figures 6b–d). As determined by large-scale DNA fragmentation assay and MTT reduction assay, we found that the knockdown of Cdk5 in cortical neurons had the neuroprotective effect (Figures 6e and f). Next, we investigated whether Cdk5-mediated phosphorylation of CHIP at Ser20 is required for these events. We found that hydrogen peroxide-induced generation of tAIF was significantly inhibited in cortical neurons overexpressing CHIP S20A as compared with CHIP WT (Figures 7a and b). We then tried to see if this was due to accelerated degradation of tAIF by UPS. Extent of hydrogen peroxide-induced generation of tAIF was quite similar in cortical neurons expressing CHIP WT or S20A in the presence of MG132 (Supplementary Figure 7).

However, tAIF ubiquitination was appeared only in cortical neurons overexpressing CHIP S20A upon exposure to hydrogen peroxide (Figure 7c), all together supporting the notion that both ubiquitination and degradation of tAIF are negatively regulated by phosphorylated CHIP at Ser20. Furthermore, large-scale DNA fragmentation assay showed that hydrogen peroxide-induced generation of 50 kbp DNA fragments was clearly detected in cortical neurons overexpressing CHIP WT, but not S20A (Figure 7d). MTT reduction assay demonstrated that hydrogen peroxide-induced cytotoxicity was significantly attenuated in cortical neurons overexpressing CHIP S20A (Figure 7e). Taken together, our present data indicate that phosphorylation of CHIP at Ser20 by activated Cdk5 is critical for promoting tAIF-mediated neuronal cell death following hydrogen peroxide treatment.

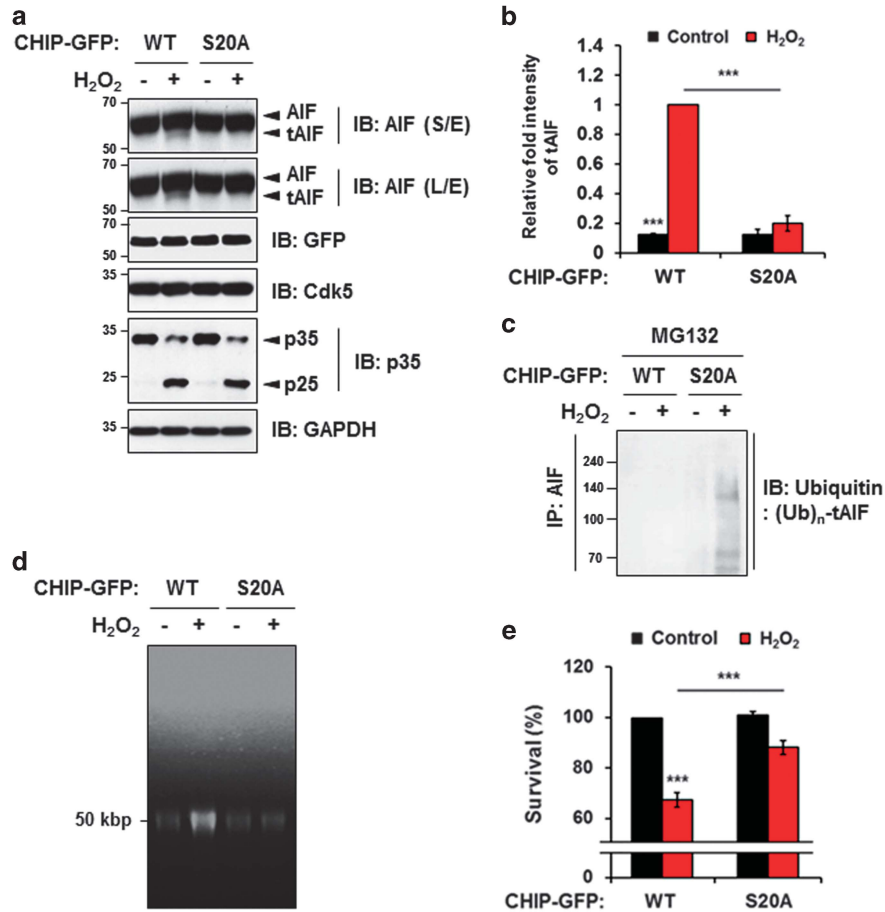


Figure 7 Cdk5-mediated phosphorylation of CHIP at Ser20 is necessary for promoting neuronal cell death via regulation of tAIF levels. (a) Cell lysates from H₂O₂ (200 μ M for 60 min)-treated or -untreated cortical neurons expressing CHIP WT-GFP or CHIP S20A-GFP were subjected to IB analysis with the indicated antibodies. S/E, short exposure; L/E, long exposure. (b) After normalization against GAPDH, relative levels of tAIF were expressed as a fold intensity over H₂O₂-treated CHIP WT-GFP controls (value = 1). Bar represents the means \pm S.D. of three independent experiments. *** P < 0.001. (c) Cortical neurons were pre-treated with 10 μ M MG132 for 4 h and further treated with 200 μ M H₂O₂ for 60 min. Cell lysates were subjected to IP using anti-AIF antibody and IB analysis using anti-Ub antibody. (d and e) Cortical neurons expressing CHIP WT-GFP or CHIP S20A-GFP were treated with or without 200 μ M H₂O₂ for 60 min and subsequently subjected to (d) the large-scale DNA fragmentation assay and (e) MTT reduction assay. Values are expressed as a percent survival over H₂O₂-untreated controls transduced with CHIP WT-GFP. Data represent the means \pm S.E.M. from three independent experiments done in triplicate. *** P < 0.001

Discussion

The fates of most cellular proteins are determined by association and dissociation cycles that coordinate the proper folding of proteins, the refolding of denatured proteins or the degradation of irreversibly damaged or toxic protein aggregates. The so-called protein triage and protein quality control system make the decision whether reactivation of proteins or their destruction will be made through the crucial cooperation of UPS, family of heat-shock protein and chaperones.⁴³ It has been demonstrated that a shared hallmark for various neurodegenerative disorders is the accumulation of toxic protein species. As UPS is the most important pathway for selective degradation of proteins, it is likely involved in progression of neurodegeneration.⁴⁴ Similarly, it has been also indicated that many of the cell death-inducing or -inhibiting proteins are targets for UPS-mediated degradation.⁴⁵ Therefore, prolonged failure and impairment in UPS have been implicated, either as a primary cause or

secondary consequences in the pathogenesis of numerous neurodegenerative disorders. In this regard, we paid attention to a CHIP protein that was originally identified as a co-chaperone of Hsc/Hsp70. CHIP has a critical regulatory role in protein quality control or stress recovery systems via its E3 ligase activity by catalyzing the immediate destruction of misfolded, impaired or toxic proteins. Recently, CHIP has been implicated in progression of the pathophysiological conditions of various neurodegenerative diseases.^{8,9,11,12,28,46,47} However, the molecular mechanisms regulating the functions of CHIP in these pathophysiological conditions are not clearly elucidated. In the present study, we identify that CHIP and Cdk5 act as critical factors to regulate the level of the toxic protein, tAIF, during oxidative stress-induced neuronal death. CHIP-mediated tAIF degradation is inhibited following the phosphorylation of CHIP by Cdk5 that is activated during hydrogen peroxide-induced neurodegeneration. More specifically, elevation of Cdk5 activity leads to increased phosphorylation of CHIP at Ser20 and this, in turn, disrupts the

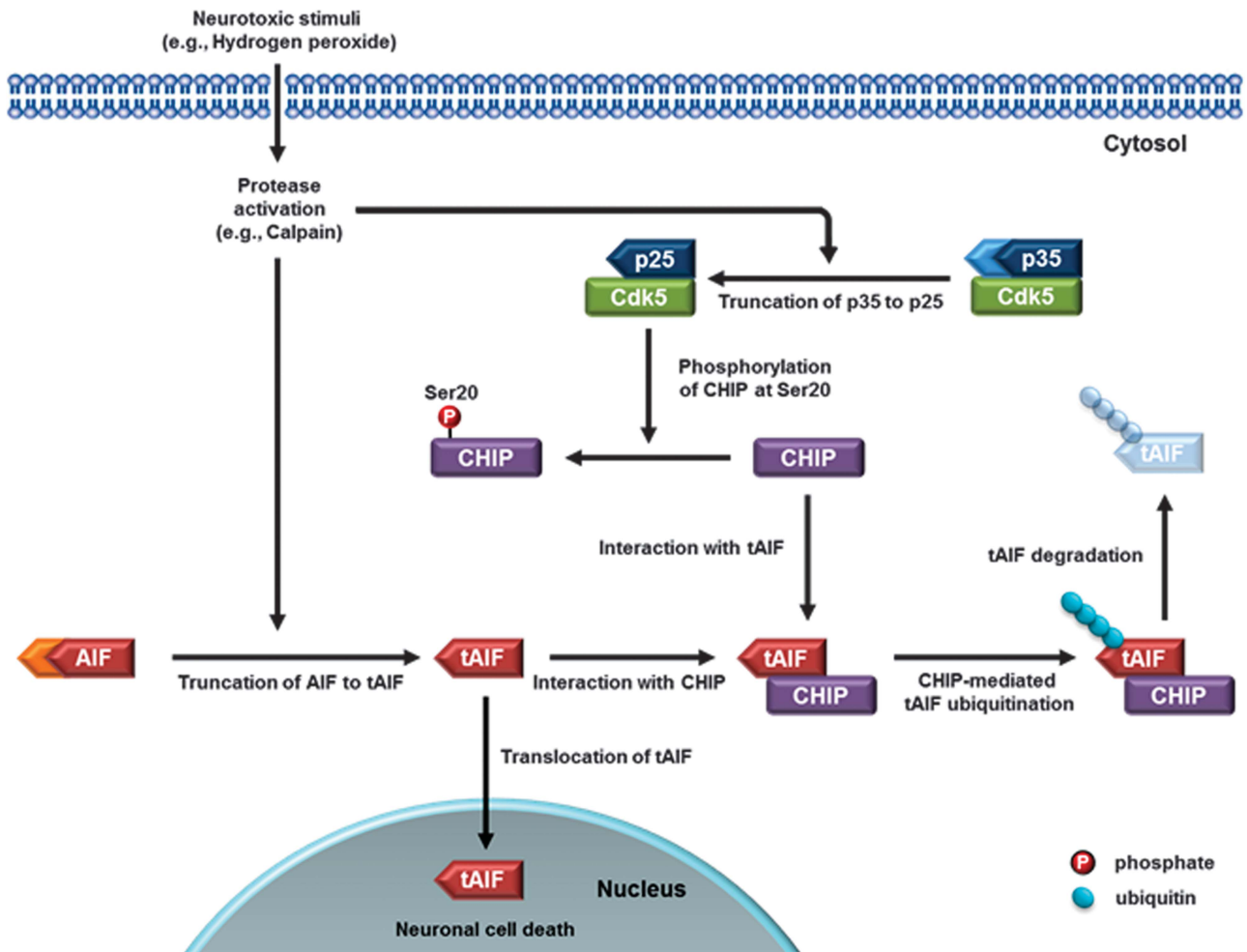


Figure 8 A model for negative regulation of tAIF by Cdk5-mediated phosphorylation of CHIP at Ser20 in response to neurotoxic stimuli. In physiological condition, CHIP mediates degradation of tAIF by UPS in the cytosol and consequently impedes tAIF-induced neuronal cell death process, which will be occurred in the nucleus. In pathophysiological conditions, however, neurotoxic stimuli including hydrogen peroxide activates calpain that are involved in truncation of p35 to p25, leading to overactivation of Cdk5 activity and subsequent phosphorylation of CHIP at Ser20 in the cytosol. This event inhibits the interaction between CHIP and tAIF in an E3 ligase-activity-independent manner. As a result, remaining tAIF is translocated into the nucleus, cleaving nuclear DNA and eventually resulting in neuronal cell death

interaction between CHIP and tAIF, eventually contributing to tAIF-mediated death in hydrogen peroxide-treated cortical neurons (Figure 8). We further confirmed whether level of tAIF is negatively regulated by degradation in the cytosol rather than by formation and release from the mitochondria following exposure to hydrogen peroxide in cortical neurons. As shown in Supplementary Figure 8, we confirm that hydrogen peroxide-induced loss of mitochondrial membrane potential and reduction of intracellular ATP level are not attenuated by cotreatment with roscovitine, suggesting that hydrogen peroxide-induced activation of Cdk5 does not cause any discernible mitochondrial damage. We also confirmed that either inhibition of Cdk5 activity (Supplementary Figure S9a) or silencing of Cdk5 (Supplementary Figure 9b) does not alter the hydrogen peroxide-induced tAIF levels in the presence of MG132. Hydrogen peroxide-induced mitochondrial release of tAIF into the cytosol and nuclear translocation concomitantly occurred (Supplementary Figure 10a) and posttreatment of roscovitine did not protect cells from

hydrogen peroxide-induced death (Supplementary Figure 11). However, hydrogen peroxide-induced release of tAIF into the cytosol and concomitant nuclear translocation are hardly detected in cortical neurons overexpressing S20A CHIP (Supplementary Figure 10b). Taken all together, these data support our conclusion that negatively regulated degradation of tAIF by Cdk5-mediated phosphorylation of CHIP is primarily responsible for determining tAIF levels in hydrogen peroxide-treated cortical neurons.

Based on previous reports demonstrating that both CHIP and Cdk5 are highly expressed in the brain and localized in the cytoplasm,^{2,9,48} we initially hypothesized mutual regulation between Cdk5 and CHIP after their direct binding: Cdk5 may phosphorylate CHIP and/or CHIP may also regulate stability of Cdk5 by UPS. However, we found that Cdk5 directly phosphorylates CHIP, whereas CHIP does not regulate the stability of Cdk5 itself (data not shown). To our knowledge, our data are the first report demonstrating that Cdk5 directly binds to and phosphorylates CHIP at Ser20. This event is, in turn,

linked to negative regulation of CHIP's function to degrade tAIF. Among many other CHIP's substrates, we also confirmed that Cdk5-mediated CHIP phosphorylation negatively regulates CHIP-mediated degradation of α -synuclein and p53 (data not shown). Previous reports indicate that kinases can phosphorylate E3 ligase to negatively or positively regulate an enzymatic activity.^{29–32} Interestingly, our present data provide a novel regulatory mechanism of CHIP by demonstrating that Cdk5-mediated phosphorylation does not decrease its E3 ligase activity. Rather, Cdk5-mediated CHIP phosphorylation causes disruption of the interaction between CHIP and its substrate, tAIF. As a consequence, tAIF escapes from CHIP-mediated degradation and is eventually linked to neurodegeneration. It would be interesting to investigate whether Cdk5-mediated CHIP phosphorylation also disrupts a physical interaction with its other known substrates without affecting its E3 ligase activity. Previously, CHIP was also observed to regulate proteasomal degradation of specific protein related with neurodegeneration in chaperone-independent manner during ER stress-induced cell death.⁴⁹ Imai *et al.* demonstrated that CHIP, Hsp70, Parkin and unfolded Pael receptor (Pael-R) form a complex and the increased level of CHIP promotes dissociation of Hsp70 from Parkin and Pael-R, thus facilitating Parkin-mediated Pael-R ubiquitination and degradation during ER stress. As a result, CHIP enhances Parkin's E3 ligase activity and thus inhibits Pael-R-induced cell death. In this regard, it would be intriguing to investigate whether CHIP phosphorylation by Cdk5 may additionally regulate Parkin's E3 ligase activity via altered binding profiles with any component of the Parkin complex and whether this represents a common regulatory mechanism involved in other ER stress-induced and non-ER stress-induced neurodegeneration as well.

It has been known that dysregulated Cdk5 activity is linked to neurodegenerative diseases including Alzheimer's disease and Parkinson's disease. Similarly, it has been demonstrated that CHIP prevents neuronal cell death through ubiquitination and subsequent degradation of its substrates including mutant superoxide dismutase 1, α -synuclein, tau, hyperphosphorylated tau, NAD(P)H:quinone oxidoreductase 1, ataxin-1 and leucine-rich repeat kinase 2 in neurodegeneration.^{22,24–28,46} However, it has not been clearly defined whether there may exist a sequential regulatory pathway between Cdk5 and CHIP governing neurodegeneration. More specifically, it has not been determined whether and how CHIP phosphorylation by activated Cdk5 regulates neuronal cell death. In this regard, another important aspect of our findings is the provision of a novel molecular mechanism for neurotoxin-induced cell death involved in neurodegeneration, where Cdk5-mediated phosphorylation of CHIP at Ser20 promotes neuronal death by inhibiting CHIP-mediated tAIF degradation. Thus, hydrogen peroxide-induced generation of tAIF was significantly inhibited in cortical neurons either by a Cdk5 shRNA or by a Cdk5 inhibitor, roscovitine. We clearly demonstrate that reduction of tAIF levels in this paradigm correlates with increased neuronal survival, as well evidenced by reduced generation of 50 kbp DNA fragments and MTT reduction assay. These phenomena were also confirmed in cortical neuron cultures treated with another neurotoxic molecule, rotenone (data not shown), suggesting that regulation of tAIF by Cdk5-mediated

phosphorylation of CHIP comprises one of the key steps to determine neuronal death. In both of cell death paradigms, neurotoxin-induced activation of Cdk5 is accompanied with a time-dependent generation of p25, potentially by activated calpain,^{50,51} leading to increased level of phosphorylated CHIP at Ser20 and concomitant appearance of tAIF. Thus, our data support the notion that neurotoxic stimuli-induced tAIF generation is critically linked to neuronal death involved in cortical neurodegeneration and this phenomenon is regulated by Cdk5-mediated phosphorylation of CHIP at Ser20. Again, our data suggest that the relationship between CHIP and dysregulated Cdk5 activation promoting neuronal death, and the potential pivotal role of CHIP and Cdk5 in neurotoxin-induced neurodegeneration. Interestingly, an assay using CIP indicate that great majority of CHIP, if not all, is phosphorylated under an unstimulated, basal condition (Supplementary Figure 12). Although it is highly speculative, we are tempting to argue that cells may recruit a distinct set of the phosphorylated CHIP by Cdk5 or unidentified protein kinases that are differentially activated depending on cellular context.

In sum, the identification of Cdk5 and CHIP as essential components involved in neurodegeneration raises the interesting possibility that these two proteins may have a critical role in other neurodegenerative diseases through the regulation of multiple pathways in neuronal cell death. Further characterization of this novel relationship between Cdk5 and CHIP will lead us to gain an improved understanding of the pathogenesis of neurodegenerative diseases and to provide a tool for developing unique therapeutic approaches.

Materials and Methods

Cell culture and treatment. HEK293 cells, HEK293T cells, SH-SY5Y neuroblastoma cells, MN9D dopaminergic neuronal cells⁵² and MEFs (kindly provided by Dr. S. Murata, Tokyo University, Tokyo, Japan) were plated on plastic culture plates (Corning Glass Works, Corning, NY, USA) or cover glasses (Marienfeld, Lauda-Konigshofen, Germany) and cultivated in Dulbecco's Modified Eagle's Medium (DMEM; Gibco, New York, NY, USA) supplemented with 10% heat-inactivated fetal bovine serum (GenDEPOT, Barker, TX, USA or Invitrogen, Carlsbad, CA, USA) in an atmosphere of either 5% CO₂ (for HEK293 cells, HEK293T cells, SH-SY5Y cells and MEF cells) or 10% CO₂ (for MN9D cells). Primary cultures of cortical neurons were prepared from gestational day 14.5 mouse embryo as previously described with some modifications.⁵³ Briefly, dissociated cortical cells were plated at densities of either 5 × 10⁶ cells per well of 6-well plate or 1 × 10⁶ cells per well of 24-well plate pre-coated with 50 μ g/ml poly-L-lysine (Sigma, St. Louis, MO, USA) and 1 μ g/ml laminin (Invitrogen), and maintained in DMEM supplemented with 2 mM glutamine (Sigma), 5% fetal bovine serum (Hyclone, South Logan, UT, USA) and 5% horse serum (Gibco) at 37 °C in humidified 5% CO₂ incubator. If necessary, cells were infected with lentivirus at 7 days *in vitro*. Chemicals added to cell cultures included roscovitine (1–20 μ M; Sigma), hydrogen peroxide (200 μ M; Calbiochem, San Diego, CA, USA) and MG132 (10 μ M; Enzo Life Sciences Inc., Farmingdale, NY, USA).

Mouse whole brain extract. The whole brain was dissected from the Ctrl: CD-1 male mice at the age of 2 weeks (Orient, Gyeonggi, Korea) in accordance with a protocol previously described⁵⁴ and homogenized in a lysis buffer (250 mM NaCl, 50 mM Tris-HCl, pH 7.4, 1 mM EDTA, 0.1% NP-40, 2 μ g/ml aprotinin, 2 μ g/ml leupeptin, 1 μ g/ml pepstatin, 5 mM NaF, 5 mM NaVO₃ and 100 μ g/ml PMSF; all from Sigma) with 1 × protease inhibitor cocktail (Roche, Basel, Switzerland) and centrifuged at 13000 × g for 15 min at 4 °C.

Plasmid construction, mutagenesis and transfection. HA-tagged CHIP and GST-HA-tagged CHIP (GST-CHIP) constructs encoding mouse CHIP were kindly provided by Dr. R Takahashi at the Kyoto University. Various CHIP mutants were generated by the site-directed mutagenesis Kit (Stratagene, La Jolla,

CA, USA) according to the manufacturer's instructions and subjected to DNA sequencing for verification. These included GST-tagged CHIP constructs (phospho-null mutants; e.g., S20A, S24A, T247A, S274A or T277A), HA- or Myc-tagged CHIP S20A constructs, HA- or Myc-tagged CHIP S20D construct (a phospho-mimetic mutant), and deletion mutants of HA-tagged CHIP constructs (e.g., Δ U-box domain lacking a.a.227–301; Δ TPR domain lacking a.a.27–128; Δ highly charged central domain lacking a.a.144–191). The Flag- or V5-tagged mouse Cdk5 WT and KD (D144N, a catalytically inactive mutant) were generated by PCR reaction and subcloned into pCI/Neo mammalian expression vector (Promega, Madison, WI, USA). Mouse Cdk5 was generated by PCR reaction and subcloned into pDsRed2. Mouse p25 was generated by PCR reaction and subcloned into pcDNA6/Myc-His or pcDNA6/V5-His. The V5-His-tagged rat tAIF and Flag-tagged Ub were kindly provided by Dr. C H Chung at the Seoul National University (Seoul, Korea) and Dr. K C Chung at the Yonsei University (Seoul, Korea), respectively. For a transient ectopic expression, eukaryotic expression plasmids were transfected into cells using either Lipofectamine 2000 (Invitrogen) or polyethylenimine (Sigma) according to the manufacturer's instructions.

Lentiviral preparation and infection. For effective transduction in primary neuronal cultures, Cdk5 knockdown for RNA interference was achieved using Mission shRNA-encoding lentivirus directed to mouse Cdk5 mRNA (Sigma; GenBank/EMBL/DBJ accession no. NM_007668) as recommended by the manufacturer's protocols. Briefly, lentiviral vectors (in pLKO.1) containing Cdk5 shRNA sequences (shCdk5 #1, TRCN0000011802; shCdk5 #2, TRCN0000278085) and non-target shRNA control vector (shScramble, SHC016) were purchased from Sigma. The lentiviral particles were generated by co-transfection into HEK293T cell with lentiviral vectors and three other vectors including pMDLg/pRRE, pMD2.G and pRSV-Rev (all from Addgene, Cambridge, MA, USA) using Lipofectamine 2000. Two days after transfection, the cell culture media were filtered using a 0.45- μ m filter (Millipore, Billerica, MA, USA). Cdk5 protein level was assessed by immunoblot analysis. Lentiviral system for overexpression was constructed by subcloning of mouse CHIP WT or S20A mutant cDNA into a *Xba*I/*Bam*HI-digested pLenti-CMV-GFP-puro vector (Addgene).

Protein purification. GST-CHIP WT and its mutant proteins were produced in *E. coli* BL21 cells after induction with 0.1 mM isopropyl- β -D-thiogalactopyranoside (Sigma) at 37 °C for 4 h. Bacterial pellets were resuspended in a lysis buffer (30 mM Tris-HCl, pH 7.5, 0.1 mM NaCl, 1% Triton X-100 (Sigma), 1 mM DTT (Sigma)) containing 1 \times protease inhibitor cocktail (Roche) and subjected to sonication on ice. The lysates were cleared by a centrifugation at 3000 \times g for 30 min at 4 °C and the supernatant was incubated at 4 °C overnight with Glutathione (GSH)-Sepharose 4B resin (Amersham Biosciences, Amersham, UK). The proteins were eluted from the resin by an elution buffer containing 50 mM Tris-HCl, pH 8.0 and 20 mM glutathione reduced ethyl ester (Sigma). The eluents were resolved by SDS-PAGE and stained with 0.1% Coomassie brilliant blue G-250 (Amresco, Solon, OH, USA) to check the purity.

Pull-down assay. The indicated lysates were incubated with GST or GST-tagged recombinant CHIP fusion protein (2 μ g per sample) at 4 °C for 3 h and precipitated by the addition of glutathione-Sepharose 4B resin. The precipitates were washed five times and subjected to immunoblot analysis using the indicated antibodies.

In vitro kinase assay. Recombinant GST-CHIP fusion protein or its mutants (3 μ g) and active Cdk5 kinase complexes (0.5 μ g, a gift from Dr. S Hisanaga at Tokyo Metropolitan University) were incubated with a kinase reaction buffer containing 40 mM Tris-HCl, pH 7.6, 2 mM DTT, 5 mM MgCl₂, 1 mM NaF, 2 mM PMSF, 0.05 mM unlabeled ATP and 5 μ Ci [γ -³²P]ATP in the presence or the absence of roscovitine (1–20 μ M) at 30 °C for 30 min. The reactants were resolved by SDS-PAGE, stained with 0.1% Coomassie brilliant blue G-250 and subjected to autoradiography. To measure endogenous Cdk5's kinase activity, immunoprecipitated Cdk5 (300 ng) obtained from cultured cortical neurons was incubated with Histone H1 protein (1 μ g, Merck Millipore, Darmstadt, Germany).

Preparation of anti-pS20 CHIP antibody. The production of anti-Ser20 CHIP phospho-specific rabbit polyclonal antibody was designed in our laboratory and generated by Abmart (Shanghai, China) using peptide C-TGGGG(pS)PDKSP surrounding the serine 20 residue on mouse CHIP.

Immunoprecipitation and immunoblot analysis. Cellular lysates were prepared using a Triton X-100 lysis buffer, consisting of 50 mM Tris-HCl, pH 7.4, 150 mM NaCl, 1 mM EDTA, 1 mM *N*-ethylmaleimide, 2 mM Na₃VO₄, 20 mM NaF, 1 mM PMSF, 1 \times protease inhibitor cocktail and 0.5% (v/v) Triton X-100. Cellular lysates were clarified by centrifugation at 13 000 \times g at 4 °C for 15 min. The resulting supernatants were subjected to immunoprecipitation and immunoblot analysis with the corresponding antibodies. When appropriate, cellular lysates were incubated at 37 °C for 1 h with 50 units of CIP (New England Biolabs, Ipswich, MA, USA) before protein separation by SDS-PAGE. For immunoprecipitation, proteins (1–3 mg) was pre-incubated with protein A agarose beads (Millipore) for pre-clearing and further incubated with 1–2 μ g of the corresponding antibodies or anti-Flag M2 affinity gel beads (Sigma) overnight at 4 °C. The immunocomplexes were collected with protein A agarose beads followed by a centrifugation at 3000 \times g at 4 °C for 2 min. Proteins were eluted from the beads by an addition of 1 \times protein sample buffer, denatured by boiling, separated on SDS-PAGE and subjected to immunoblot analysis. Antibodies used included anti-HA antibody (Santa Cruz Biotechnology, Dallas, TX, USA), anti-CHIP antibody (Santa Cruz), anti-Cdk5 antibody (Santa Cruz), anti-AIF (Santa Cruz), anti-p35 (Santa Cruz), horseradish peroxidase (HRP)-conjugated anti-HA (Roche Applied Science), HRP-conjugated anti-Flag antibody (Sigma), anti-V5 antibody (Invitrogen), anti-c-Myc antibody (Cell Signaling, Beverly, MA, USA), anti-GFP antibody (Santa Cruz), anti-Ub antibody (Santa Cruz), anti-glyceraldehyde-3-phosphate dehydrogenase antibody (Millipore), anti-actin antibody (Sigma), HRP-conjugated anti-mouse or rabbit antibodies (Santa Cruz) and HRP-conjugated anti-goat antibody (Abcam, Cambridge, UK). Enhanced chemiluminescence (Amersham Bioscience) was used to detect specific bands. The relative band intensity was measured using Image J imaging software (National Institutes of Health, Bethesda, MD, USA).

Fluorescence microscopy. For immunofluorescence localization of the target molecules, HEK293 cells were cultured on cover glasses and co-transfected with HA-CHIP WT and DsRed2-tagged Cdk5 constructs. At 48 h post-transfection, cells were fixed with 4% paraformaldehyde (Electron Microscopy Sciences, Hatfield, PA, USA) and blocked for 1 h at RT in PBS (Lonza, Basel, Switzerland) containing 5% normal goat serum (Invitrogen) and 0.2% Triton X-100. Cells were then incubated with a mouse monoclonal anti-HA antibody overnight at 4 °C followed by incubation with Alexa Fluor 488-conjugated goat anti-mouse IgG (Invitrogen). Fluorescence images were observed under an LSM 510 META confocal laser scanning microscope equipped with epifluorescence and a LSM digital image analyzer (Carl Zeiss, Jena, Germany). Hoechst 33258 (Molecular Probes, Eugene, OR, USA) was used as a counter staining probe to mark the nuclei.

Ubiquitination assay. *In vitro* auto-ubiquitination assay was performed as described previously with some modifications in a reaction buffer containing 50 mM Tris-HCl, pH 7.6, 4 mM ATP, 2 mM MgCl₂ and 1 mM DTT.⁵⁵ In brief, after *in vitro* kinase assays with 2 mM unlabeled ATP, the reactants were pre-incubated with 1 μ g/ μ l ubiquitin aldehyde (Calbiochem) at 37 °C for 5 min and further incubated with recombinant GST-CHIP fusion protein, 100 ng UBE1 (E1 enzyme; Boston Biochem), 500 ng UbcH5b (E2 enzyme; Boston Biochem, Cambridge, UK) and 6 μ g Ub (Calbiochem) at 30 °C for 2 h and then terminated by addition of 5 \times protein sample buffer and boiling, followed by immunoblot analysis using anti-CHIP and anti-Ub antibodies. For a cell-based *in vivo* ubiquitination assay, cells were incubated with 10 μ M MG132 and lysed in a lysis buffer. Cell lysates were subjected to immunoprecipitation followed by immunoblot analysis with the corresponding antibodies. Cell-based *in vivo* auto-ubiquitination assay by denature IP was performed as described previously with some modifications.⁵⁶ To disrupt non-covalent protein–protein interactions, lysates were heated at 98 °C in a lysis buffer containing 1% SDS.

Cell death assessment. Rate of cell survival was determined by the MTT reduction assay as previously described with some modifications.⁵⁷ Briefly, cortical neurons cultured on a 24-well plate were incubated with 1 mg/ml MTT solution at 37 °C for 1 h and lysed in a buffer containing in 20% SDS and 50% aqueous dimethylformamide for 24 h. The optical density of the dissolved formazan grains was measured at 595 and 650 nm as a test and a reference wavelength, respectively, using a VICTOR X3 multilabel plate reader (Perkin Elmer, Waltham, MA, USA).

Genomic DNA isolation and DNA fragmentation assessment. Total genomic DNA was extracted from cortical neurons using the AccuPrep

Genomic DNA Extraction Kit (Bioneer, Daejeon, Korea) according to the manufacturer's instruction. Large-scale DNA fragmentation assessment was performed as previously described with some modifications.⁵⁸ Briefly, extracted DNA fragments were separated in a 1.0% agarose gel by a pulsed-field gel electrophoresis using a CHEF-DR111 system (Bio-Rad) at 6 V/cm for 20 h at an angle of 120°, with switching times ramped from 5 to 50 s at 14 °C. The gel was stained with ethidium bromide and visualized under a UV light.

Statistics. The data were expressed as the means \pm S.D. or the means \pm S.E. M. Significance between groups was determined by one-way analysis of variance and the Tukey's *post hoc* test using GraphPad Prism 6 (La Jolla, CA, USA). Values of *** P < 0.001, ** P < 0.01 or * P < 0.05 were considered statistically significant.

Conflict of Interest

The authors declare no conflict of interest.

Acknowledgements. This work was supported by the National Research Foundation of Korea (NRF) grant through SRC (2008-0061888; YJO), by the Ministry for Health, Welfare and Family Affairs (A111382; YJO, and by a grant from the Ministry of Science, ICT and Future Planning (2012R1A2A1A03010177; to P-LH).

- Dhavan R, Tsai LH. A decade of CDK5. *Nat Rev Mol Cell Biol* 2001; **2**: 749–759.
- Cheung ZH, Ip NY. Cdk5: mediator of neuronal death and survival. *Neurosci Lett* 2004; **361**: 47–51.
- Smith DS, Greer PL, Tsai LH. Cdk5 on the brain. *Cell Growth Differ* 2001; **12**: 277–283.
- Cheung ZH, Fu AK, Ip NY. Synaptic roles of Cdk5: implications in higher cognitive functions and neurodegenerative diseases. *Neuron* 2006; **50**: 13–18.
- Patrick GN, Zukerberg L, Nikolic M, de la Monte S, Dikkes P, Tsai LH. Conversion of p35 to p25 deregulates Cdk5 activity and promotes neurodegeneration. *Nature* 1999; **402**: 615–622.
- Cheung ZH, Ip NY. Cdk5: a multifaceted kinase in neurodegenerative diseases. *Trends Cell Biol* 2012; **22**: 169–175.
- Su SC, Tsai LH. Cyclin-dependent kinases in brain development and disease. *Annu Rev Cell Dev Biol* 2011; **27**: 465–491.
- McDonough H, Patterson C. CHIP: a link between the chaperone and proteasome systems. *Cell Stress Chaperones* 2003; **8**: 303–308.
- Ballinger CA, Connell P, Wu Y, Hu Z, Thompson LJ, Yin LY *et al*. Identification of CHIP, a novel tetratricopeptide repeat-containing protein that interacts with heat shock proteins and negatively regulates chaperone functions. *Mol Cell Biol* 1999; **19**: 4535–4545.
- Jiang J, Ballinger CA, Wu Y, Dai Q, Cyr DM, Hohfeld J *et al*. CHIP is a U-box-dependent E3 ubiquitin ligase: identification of Hsc70 as a target for ubiquitylation. *J Biol Chem* 2001; **276**: 42938–42944.
- Dickey CA, Patterson C, Dickson D, Petrucelli L. Brain CHIP: removing the culprits in neurodegenerative disease. *Trends Mol Med* 2007; **13**: 32–38.
- Qian SB, McDonough H, Boellmann F, Cyr DM, Patterson C. CHIP-mediated stress recovery by sequential ubiquitination of substrates and Hsp70. *Nature* 2006; **440**: 551–555.
- Murata S, Minami Y, Minami M, Chiba T, Tanaka K. CHIP is a chaperone-dependent E3 ligase that ubiquitylates unfolded protein. *EMBO Rep* 2001; **2**: 1133–1138.
- Sahara N, Murayama M, Mizoroki T, Urushitani M, Imai Y, Takahashi R *et al*. *In vivo* evidence of CHIP up-regulation attenuating tau aggregation. *J Neurochem* 2005; **94**: 1254–1263.
- Dai Q, Zhang C, Wu Y, McDonough H, Whaley RA, Godfrey V *et al*. CHIP activates HSF1 and confers protection against apoptosis and cellular stress. *EMBO J* 2003; **22**: 5446–5458.
- Kumar P, Ambasta RK, Veereshwarayya V, Rosen KM, Kosik KS, Band H *et al*. CHIP and HSPs interact with beta-APP in a proteasome-dependent manner and influence Abeta metabolism. *Hum Mol Genet* 2007; **16**: 848–864.
- Gao Y, Han C, Huang H, Xin Y, Xu Y, Luo L *et al*. Heat shock protein 70 together with its co-chaperone CHIP inhibits TNF-alpha induced apoptosis by promoting proteasomal degradation of apoptosis signal-regulating kinase1. *Apoptosis* 2010; **15**: 822–833.
- Kampinga HH, Kanon B, Salomons FA, Kabakov AE, Patterson C. Overexpression of the co-chaperone CHIP enhances Hsp70-dependent folding activity in mammalian cells. *Mol Cell Biol* 2003; **23**: 4948–4958.
- Furuya T, Kim M, Lipinski M, Li J, Kim D, Lu T *et al*. Negative regulation of Vps34 by Cdk mediated phosphorylation. *Mol Cell* 2010; **38**: 500–511.
- Wong AS, Lee RH, Cheung AY, Yeung PK, Chung SK, Cheung ZH *et al*. Cdk5-mediated phosphorylation of endophilin B1 is required for induced autophagy in models of Parkinson's disease. *Nat Cell Biol* 2011; **13**: 568–579.
- Contreras-Vallejos E, Utreras E, Gonzalez-Billault C. Going out of the brain: non-nervous system physiological and pathological functions of Cdk5. *Cell Signal* 2012; **24**: 44–52.
- Shin Y, Klucken J, Patterson C, Hyman BT, McLean PJ. The co-chaperone carboxyl terminus of Hsp70-interacting protein (CHIP) mediates alpha-synuclein degradation decisions between proteasomal and lysosomal pathways. *J Biol Chem* 2005; **280**: 23727–23734.
- Kumar P, Pradhan K, Karunya R, Ambasta RK, Querfurth HW. Cross-functional E3 ligases Parkin and C-terminus Hsp70-interacting protein in neurodegenerative disorders. *J Neurochem* 2012; **120**: 350–370.
- Urushitani M, Kurisu J, Tateno M, Hatakeyama S, Nakayama K, Kato S *et al*. CHIP promotes proteasomal degradation of familial ALS-linked mutant SOD1 by ubiquitinating Hsp/Hsc70. *J Neurochem* 2004; **90**: 231–244.
- Tsvetkov P, Adamovich Y, Elliott E, Shaul Y. E3 ligase STUB1/CHIP regulates NAD(P)H: quinone oxidoreductase 1 (NQO1) accumulation in aged brain, a process impaired in certain Alzheimer disease patients. *J Biol Chem* 2011; **286**: 8839–8845.
- Al-Ramahi I, Lam YC, Chen HK, de Gouyon B, Zhang M, Perez AM *et al*. CHIP protects from the neurotoxicity of expanded and wild-type ataxin-1 and promotes their ubiquitination and degradation. *J Biol Chem* 2006; **281**: 26714–26724.
- Ko HS, Bailey R, Smith WW, Liu Z, Shin JH, Lee YI *et al*. CHIP regulates leucine-rich repeat kinase-2 ubiquitination, degradation, and toxicity. *Proc Natl Acad Sci USA* 2009; **106**: 2897–2902.
- Oh KH, Yang SW, Park JM, Seol JH, Iemura S, Natsume T *et al*. Control of AIF-mediated cell death by antagonistic functions of CHIP ubiquitin E3 ligase and USP2 deubiquitinating enzyme. *Cell Death Differ* 2011; **18**: 1326–1336.
- Avraham E, Rott R, Liani E, Szargel R, Engelender S. Phosphorylation of Parkin by the cyclin-dependent kinase 5 at the linker region modulates its ubiquitin-ligase activity and aggregation. *J Biol Chem* 2007; **282**: 12842–12850.
- Ko HS, Lee Y, Shin JH, Karuppagounder SS, Gadad BS, Koleske AJ *et al*. Phosphorylation by the c-Abl protein tyrosine kinase inhibits parkin's ubiquitination and protective function. *Proc Natl Acad Sci USA* 2010; **107**: 16691–16696.
- Yang C, Zhou W, Jeon MS, Demydenko D, Harada Y, Zhou H *et al*. Negative regulation of the E3 ubiquitin ligase itch via Fyn-mediated tyrosine phosphorylation. *Mol Cell* 2006; **21**: 135–141.
- Nacerdine K, Beaudry JB, Ginjala V, Westerman B, Mattioli F, Song JY *et al*. Akt-mediated phosphorylation of Brmi1 modulates its oncogenic potential, E3 ligase activity, and DNA damage repair activity in mouse prostate cancer. *J Clin Invest* 2012; **122**: 1920–1932.
- Hao B, Oehmann S, Sowa ME, Harper JW, Pavletich NP. Structure of a Fbw7-Skp1-cyclin E complex: multisite-phosphorylated substrate recognition by SCF ubiquitin ligases. *Mol Cell* 2007; **26**: 131–143.
- Feldman RM, Correll CC, Kaplan KB, Deshaies RJ. A complex of Cdc4p, Skp1p, and Cdc53p/cullin catalyzes ubiquitination of the phosphorylated CDK inhibitor Sic1p. *Cell* 1997; **91**: 221–230.
- Skowyra D, Craig KL, Tyers M, Elledge SJ, Harper JW. F-box proteins are receptors that recruit phosphorylated substrates to the SCF ubiquitin-ligase complex. *Cell* 1997; **91**: 209–219.
- Verma R, Annan RS, Huddleston MJ, Carr SA, Reynard G, Deshaies RJ. Phosphorylation of Sic1p by G1 Cdk required for its degradation and entry into S phase. *Science* 1997; **278**: 455–460.
- Shelton SB, Johnson GV. Cyclin-dependent kinase-5 in neurodegeneration. *J Neurochem* 2004; **88**: 1313–1326.
- Gong X, Tang X, Wiedmann M, Wang X, Peng J, Zheng D *et al*. Cdk5-mediated inhibition of the protective effects of transcription factor MEF2 in neurotoxicity-induced apoptosis. *Neuron* 2003; **38**: 33–46.
- Son YO, Jang YS, Heo JS, Chung WT, Choi KC, Lee JC. Apoptosis-inducing factor plays a critical role in caspase-independent, pyknotic cell death in hydrogen peroxide-exposed cells. *Apoptosis* 2009; **14**: 796–808.
- Klein JA, Longo-Guess CM, Rossmann MP, Seburn KL, Hurd RE, Frankel WN *et al*. The harlequin mouse mutation downregulates apoptosis-inducing factor. *Nature* 2002; **419**: 367–374.
- Cheung EC, Melanson-Drapeau L, Cregan SP, Vanderluit JL, Ferguson KL, McIntosh WC *et al*. Apoptosis-inducing factor is a key factor in neuronal cell death propagated by BAX-dependent and BAX-independent mechanisms. *J Neurosci* 2005; **25**: 1324–1334.
- Cregan SP, Fortin A, MacLaurin JG, Callaghan SM, Ceconi F, Yu SW *et al*. Apoptosis-inducing factor is involved in the regulation of caspase-independent neuronal cell death. *J Cell Biol* 2002; **158**: 507–517.
- Wickner S, Maurizi MR, Gottesman S. Posttranslational quality control: folding, refolding, and degrading proteins. *Science* 1999; **286**: 1888–1893.
- Dennissen FJ, Kholod N, van Leeuwen FW. The ubiquitin proteasome system in neurodegenerative diseases: culprit, accomplice or victim? *Prog Neurobiol* 2012; **96**: 190–207.
- Vucic D, Dixit VM, Wertz IE. Ubiquitylation in apoptosis: a post-translational modification at the edge of life and death. *Nat Rev Mol Cell Biol* 2011; **12**: 439–452.

46. Shimura H, Schwartz D, Gygi SP, Kosik KS. CHIP-Hsc70 complex ubiquitinates phosphorylated tau and enhances cell survival. *J Biol Chem* 2004; **279**: 4869–4876.
47. Connell P, Ballinger CA, Jiang J, Wu Y, Thompson LJ, Hohfeld J *et al*. The co-chaperone CHIP regulates protein triage decisions mediated by heat-shock proteins. *Nat Cell Biol* 2001; **3**: 93–96.
48. Tsai LH, Takahashi T, Caviness VS Jr, Harlow E. Activity and expression pattern of cyclin-dependent kinase 5 in the embryonic mouse nervous system. *Development* 1993; **119**: 1029–1040.
49. Imai Y, Soda M, Hatakeyama S, Akagi T, Hashikawa T, Nakayama KI *et al*. CHIP is associated with Parkin, a gene responsible for familial Parkinson's disease, and enhances its ubiquitin ligase activity. *Mol Cell* 2002; **10**: 55–67.
50. Lee MS, Kwon YT, Li M, Peng J, Friedlander RM, Tsai LH. Neurotoxicity induces cleavage of p35 to p25 by calpain. *Nature* 2000; **405**: 360–364.
51. Camins A, Verdaguer E, Folch J, Pallas M. Involvement of calpain activation in neurodegenerative processes. *CNS Drug Rev* 2006; **12**: 135–148.
52. Choi HK, Won LA, Kontur PJ, Hammond DN, Fox AP, Wainer BH *et al*. immortalization of embryonic mesencephalic dopaminergic neurons by somatic cell fusion. *Brain Res* 1991; **552**: 67–76.
53. Koh JY, Gwag BJ, Lobner D, Choi DW. Potentiated necrosis of cultured cortical neurons by neurotrophins. *Science* 1995; **268**: 573–575.
54. Jackson-Lewis V, Przedborski S. Protocol for the MPTP mouse model of Parkinson's disease. *Nat Protoc* 2007; **2**: 141–151.
55. Murata S, Minami M, Minami Y. Purification and assay of the chaperone-dependent ubiquitin ligase of the carboxyl terminus of Hsc70-interacting protein. *Methods Enzymol* 2005; **398**: 271–279.
56. Nagai H, Noguchi T, Homma K, Katagiri K, Takeda K, Matsuzawa A *et al*. Ubiquitin-like sequence in ASK1 plays critical roles in the recognition and stabilization by USP9X and oxidative stress-induced cell death. *Mol Cell* 2009; **36**: 805–818.
57. Takuma K, Fang F, Zhang W, Yan S, Fukuzaki E, Du H *et al*. RAGE-mediated signaling contributes to intraneuronal transport of amyloid-beta and neuronal dysfunction. *Proc Natl Acad Sci USA* 2009; **106**: 20021–20026.
58. Yuste VJ, Sanchez-Lopez I, Sole C, Moubarak RS, Bayascas JR, Dolcet X *et al*. The contribution of apoptosis-inducing factor, caspase-activated DNase, and inhibitor of caspase-activated DNase to the nuclear phenotype and DNA degradation during apoptosis. *J Biol Chem* 2005; **280**: 35670–35683.

Supplementary Information accompanies this paper on Cell Death and Differentiation website (<http://www.nature.com/cdd>)